

Cite this: *Chem. Sci.*, 2021, 12, 10605

All publication charges for this article have been paid for by the Royal Society of Chemistry

Oxygen atom transfer promoted nitrate to nitric oxide transformation: a step-wise reduction of nitrate \rightarrow nitrite \rightarrow nitric oxide†

Kulbir,^a Sandip Das,^a Tarali Devi,^c Mrigaraj Goswami,^a Mahesh Yenuganti,^a Prabhakar Bhardwaj,^a Somnath Ghosh,^a Subash Chandra Sahoo^b and Pankaj Kumar^{a*}

Nitrate reductases (NRs) are molybdoenzymes that reduce nitrate (NO_3^-) to nitrite (NO_2^-) in both mammals and plants. In mammals, the salivary microbes take part in the generation of the NO_2^- from NO_3^- , which further produces nitric oxide (NO) either in acid-induced NO_2^- reduction or in the presence of nitrite reductases (NiRs). Here, we report a new approach of VCl_3 (V^{3+} ion source) induced step-wise reduction of NO_3^- in a Co^{II} -nitrate complex, $[(12\text{-TMC})\text{Co}^{\text{II}}(\text{NO}_3^-)]^+$ (**2**, $\{\text{Co}^{\text{II}}-\text{NO}_3^-\}$), to a Co^{III} -nitrosyl complex, $[(12\text{-TMC})\text{Co}^{\text{III}}(\text{NO})]^{2+}$ (**4**, $\{\text{CoNO}\}^8$), bearing an *N*-tetramethylated cyclam (TMC) ligand. The VCl_3 inspired reduction of NO_3^- to NO is believed to occur in two consecutive oxygen atom transfer (OAT) reactions, i.e., $\text{OAT-1} = \text{NO}_3^- \rightarrow \text{NO}_2^-$ (r_1) and $\text{OAT-2} = \text{NO}_2^- \rightarrow \text{NO}$ (r_2). In these OAT reactions, VCl_3 functions as an O-atom abstracting species, and the reaction of **2** with VCl_3 produces a Co^{III} -nitrosyl ($\{\text{CoNO}\}^8$) with V^{V} -Oxo ($\{\text{V}^{\text{V}}=\text{O}\}^{3+}$) species, via a proposed Co^{II} -nitrito (**3**, $\{\text{Co}^{\text{II}}-\text{NO}_2^-\}$) intermediate species. Further, in a separate experiment, we explored the reaction of isolated complex **3** with VCl_3 , which showed the generation of **4** with V^{V} -Oxo, validating our proposed reaction sequences of OAT reactions. We ensured and characterized **3** using VCl_3 as a limiting reagent, as the second-order rate constant of OAT-2 (k_2') is found to be ~ 1420 times faster than that of the OAT-1 (k_2) reaction. Binding constant (K_b) calculations also support our proposition of NO_3^- to NO transformation in two successive OAT reactions, as $K_{b(\text{Co}^{\text{II}}-\text{NO}_2^-)}$ is higher than $K_{b(\text{Co}^{\text{II}}-\text{NO}_3^-)}$, hence the reaction moves in the forward direction (OAT-1). However, $K_{b(\text{Co}^{\text{II}}-\text{NO}_2^-)}$ is comparable to $K_{b(\text{CoNO})}^8$, and therefore sequenced the second OAT reaction (OAT-2). Mechanistic investigations of these reactions using ^{15}N -labeled- $^{15}\text{NO}_3^-$ and $^{15}\text{NO}_2^-$ revealed that the N-atom in the $\{\text{CoNO}\}^8$ is derived from NO_3^- ligand. This work highlights the first-ever report of VCl_3 induced step-wise NO_3^- reduction (NRs activity) followed by the OAT induced NO_2^- reduction and then the generation of Co-nitrosyl species $\{\text{CoNO}\}^8$.

Received 9th February 2021

Accepted 1st July 2021

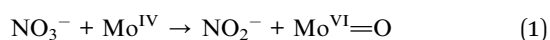
DOI: 10.1039/d1sc00803j

rsc.li/chemical-science

Introduction

The mechanism of microbial denitrification is still one of the most mysterious subjects, despite being explored in detail in both *in vivo* and *in vitro* systems. Based on the extensive research and literature available, denitrification has been well accepted to be a four-step reductive process of nitrate (NO_3^-) to dinitrogen (N_2) conversion $\{\text{NO}_3^- \rightarrow \text{NO}_2^- \rightarrow \text{NO} \rightarrow \text{N}_2\text{O} \rightarrow$

$\text{N}_2\}$, through a series of intermediate gaseous nitrogen oxide products.¹ In mammals and bacteria, inorganic NO_3^- and nitrite (NO_2^-) serve as a fundamental storage material of NO for its bio-physiological processes.^{2,3} However, in humans, an excessive amount of NO_3^- has been discovered to cause gastric cancer and other disorders.⁴ To maintain an optimal NO_3^- level in the bio-system, commensal bacteria in the human oral cavity play a vital role in converting NO_3^- to NO_2^- (eqn (1)).² In bacteria, molybdenum-based nitrate reductase (NRs) enzymes generate NO_2^- via an OAT reaction from NO_3^- anion.⁵ At the bio-physiological level, NO_2^- serves as a pool of NO and can easily be transformed to NO, either (i) in non-enzymatic acid-catalyzed NO_2^- reduction in the stomach^{6,7} or (ii) by Fe and Cu based nitrite reductase (NiRs) enzymes catalyzed reactions (eqn (2)).^{8,9}



^aDepartment of Chemistry, Indian Institute of Science Education and Research (IISER), Tirupati 517507, India. E-mail: pankajatiisert@gmail.com; pankaj@iisertirupati.ac.in

^bDepartment of Chemistry, Punjab University, Chandigarh, Punjab, India

^cHumboldt-Universität zu Berlin, Institut für Chemie, Brook-Taylor-Straße 2, D-12489 Berlin, Germany

† Electronic supplementary information (ESI) available: For the Experimental details. CCDC 2058406 and 2058407. For ESI and crystallographic data in CIF or other electronic format see DOI: 10.1039/d1sc00803j



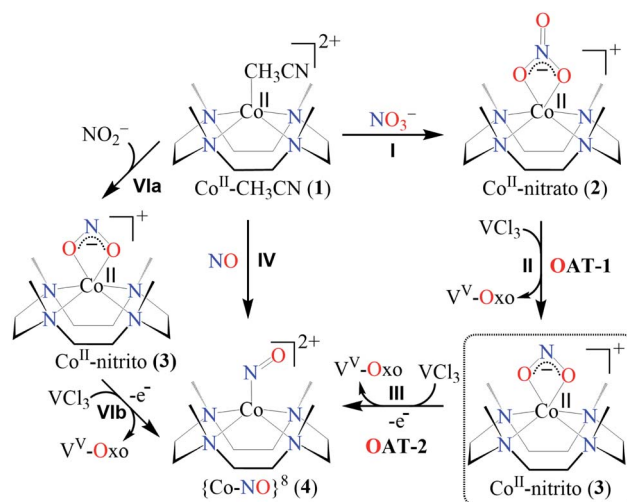
NO is a gaseous secondary messenger in animals, plants, fungi, and bacteria. In plants, NO is involved in different physiological processes, such as plant growth & development, metabolism, aging, defense against pathogens, biotic and abiotic trauma.¹⁰ However, NO regulates various physiological processes in mammals.¹¹ For instance, NO inadequacy possibly will aggravate the pathogenic effects associated with atherosclerosis, diabetic hypertension, *etc.*¹² Also, the immune response of NO towards the harmful pathogens is related to the oxidized NO species,¹³ *i.e.*, peroxynitrite (PN, ONOO^-)^{13a,14} or nitrogen dioxide (NO_2).^{15,16} Hence, balanced production of NO is required to maintain a normal homeostatic bio-physiological condition. In bio-systems, enzymes, *i.e.*, NiRs^{8,9,17} and endothelial nitric oxide synthases (eNOSs)^{17,18} are available for NO generation. The NOSs enzymes catalyze the biosynthesis of NO from L-arginine.¹⁸

In the case of NO overproduction, nitric oxide dioxygenase (NODs) generates NO_3^- in the reaction of the iron-dioxygen adduct with NO *via* a proposed PN intermediate,¹⁹ as explored in other biomimetic systems.^{19d,20} Also, there are various reports on NO_2^- formation in nitric oxide monooxygenation (NOM) reaction from metal-nitrosyls in the presence of O_2 , $\text{O}_2^{\cdot-}$ and OH^- .^{19a,20b,21} Oxidized species of NO (NO_3^- & NO_2^-) may also generate *via* different oxidative processes (*vide supra*). However, NO_3^- to NO_2^- transformation and $\text{NO}_3^-/\text{NO}_2^-$ to NO conversion (*vide versa*) are critical steps of the denitrification process.¹

In an attempt to mimic the denitrification process, R. H. Holm and co-workers reported NRs activity, molybdenum, and tungsten-based catalyst for catalytic reduction of NO_3^- to NO_2^- with metal-Oxo species.²² Similarly, S. Sarkar and co-workers have reported Mo^{IV} mediated reduction of NO_3^- to NO_2^- to mimic NRs activity.²³ Eunsuk Kim proposed the reduction of NO_3^- to NO_2^- using the Lewis acid Sc^{3+} to activate the OAT reaction from NO_3^- to Mo metal center.²⁴ On the other hand, nitrite reduction chemistry is explored widely; Ford and co-workers examined the acid-induced reduction of NO_2^- to N_2O in a Fe-porphyrin complex.²⁵ Warren group described the NiR by using the thiol group.²⁶ Recently, we have reported acid-induced nitrite reduction to NO.²⁷ However, the conversion of NO_3^- to NO using a single catalyst is barely explored; Yunho Lee and co-workers testified Ni catalyzed the transformation of inorganic NO_3^- to N_2 *via* NO_2^- intermediate using the carbon monoxide (CO) as oxophilic species.²⁸

In biological systems^{3,5a} and biomimetic^{22,23,27,29} or catalytic reactions,²⁴ the approach towards converting NO_3^- to NO is usually a two-enzymes/-catalysts-induced two-step process in two different reactions (*i.e.*, NO_3^- reduction followed by NO_2^-

reduction).^{5a} However, only a few reports simultaneously carry out both the NO_3^- and NO_2^- reduction using a single metal center in a biomimetic system. Here, our eagerness is to mimic the NRs enzymatic reaction followed by the NO_2^- reduction, sponsored by the same reagent (*i.e.*, single metal-induced two-step NO_3^- to NO conversion). Herein, we report the NO_3^- reduction chemistry of a $\text{Co}^{\text{II}}\text{-NO}_3^-$ complex, $[(12\text{-TMC})\text{Co}^{\text{II}}(\text{NO}_3)]^+$ (2), bearing a 12-TMC ligand (12-TMC = 1,4,7,10-tetramethyl-1,4,7,10-tetraazacyclododecane) *via* the two consecutive oxygen atom transfer (OAT) reactions using VCl_3 as an oxophilic compound (Scheme 1, reaction II & III). Complex 2 reacts with VCl_3 to form corresponding Co^{III} -nitrosyl complex, $[(12\text{-TMC})\text{Co}^{\text{III}}(\text{NO})]^{2+}$ (ref. 19d, 20b, 21a, 27 and 30) (4), with $\text{V}^{\text{V}}\text{-Oxo}$ ($\{\text{V}^{\text{V}}=\text{O}\}^{3+}$) species, which further decomposes to V_2O_5 , *via* the formation of a presumed Co^{II} -nitrito ($3, \{\text{Co}^{\text{II}}\text{-NO}_2^-\}$) intermediate in MeOH or H_2O at 298 K (Scheme 1, reaction II). Interpretation of various spectral measurements, we have confirmed the generation of 3 with $\text{V}^{\text{V}}\text{-Oxo}$ by the transfer of one O-atom from NO_3^- moiety of 2 to VCl_3 (OAT-1). Further, we observed the generation of 4 with $\text{V}^{\text{V}}\text{-Oxo}$ from 3 upon reaction with VCl_3 (OAT-2), under similar reaction conditions, showing the similar OAT induced NO_2^- reduction reactivity as reported in the case of PPh_3 and sulphur based compounds (thiols and thioethers) (eqn (3)–(6)).^{26,31} Combining these two OAT reactions, we can predict the reaction sequences, *i.e.*, the first OAT from NO_3^- moiety of 2 to VCl_3 and the generation of 3, {OAT-1 = $\text{Co}^{\text{II}}\text{-NO}_3^- + \text{VCl}_3 \rightarrow \text{Co}^{\text{II}}\text{-NO}_2^- + \text{VOCl}_3$ (r_1)}. Subsequently, the second OAT from NO_2^- moiety of 3 to another VCl_3 moiety and the generation of 4 {OAT-2 = $\text{Co}^{\text{II}}\text{-NO}_2^- + \text{VCl}_3 \rightarrow \{\text{CoNO}\}^8 + \text{VOCl}_3$ (r_2)}. Mechanistic investigation using ^{15}N -labeled- $^{15}\text{NO}_3^-$ & $^{15}\text{NO}_2^-$ confirmed clearly that the N-atom in the $\{\text{CoNO}\}^8$ is derived from NO_3^- anion of 2. To the best of our knowledge, the present work reports the first example of VCl_3 induced conversion of $\text{Co}^{\text{II}}\text{-NO}_3^-$ to $\{\text{CoNO}\}^8$ in two successive OAT reactions, demonstrating a new mechanistic approach for one-metal induced NO_3^- to NO_2^- reduction (NRs activity) followed by NO_2^- to NO conversion (OAT induced NO_2^- reduction).



Scheme 1



Results and discussion

Preparation of Co^{II}-nitrate complex, [(12-TMC)Co^{II}(NO₃[−])]⁺ (2)

The primary Co^{II}-nitrate complex, [(12-TMC)Co^{II}(NO₃[−])]⁺ (2), was prepared by reacting Co^{II}-complex, [(12-TMC)Co^{II}(NCCH₃)]²⁺ (1), with 1 equivalent of NaNO₃ in H₂O/CH₃CN (Scheme 1, the reaction I; also see ESI† and Experimental section (ES)). Further, 2 was characterized by various spectroscopic techniques, including the single-crystal X-ray structure determination. UV-vis absorption band of 1 ($\lambda_{\text{max}} = 485$ nm) changed to a new band ($\lambda_{\text{max}} = 480$ nm, $\epsilon = 25 \text{ M}^{-1} \text{ cm}^{-1}$) upon addition of 1 equivalent NaNO₃ in CH₃CN at RT, suggesting the formation of 2 (Fig. 1a). FT-IR spectrum of 2 showed a characteristic peak for Co^{II}-bound NO₃[−] anion at 1384 cm^{−1} and shifted to 1358 cm^{−1} when exchanged with ¹⁵N-labeled-NO₃[−] (¹⁵N¹⁶O₃[−]) (Fig. 1a; ESI, Fig. S1†). A wide range ¹H-NMR spectrum of 2 showed fairly clean paramagnetic proton-signals (Figure S2a†), suggesting a magnetically active Co-center. The spin state of 2 was determined by calculating the magnetic moment of the Co^{II} metal-center by the Evans' method and found to be 4.46 BM, suggesting a high spin Co^{II}-ion in complex 2 (ES, ESI, Fig. S2b†). Electrospray ionization mass spectrum (ESI-MS) of 2 showed a prominent peak at m/z 349.1, which shifted to m/z 350.1 when prepared with ¹⁵N-labeled Na¹⁵NO₃, and their mass and isotope distribution pattern corresponds to [(12-TMC)Co^{II}(¹⁴NO₃)]⁺ (calc. m/z 349.1) and [(12-TMC)Co^{II}(¹⁵NO₃)]⁺ (calc. m/z 350.1), respectively (Fig. 1a; ESI, Fig. S3†). In addition to the above experimental characterization, 2 was structurally characterized by single-crystal X-ray crystallography. Complex 2 has a six-coordinate distorted octahedral geometry around the Co^{II}-center, possessing O, O[−]-

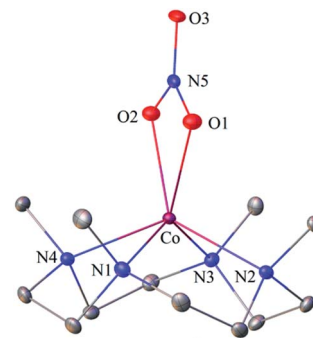


Fig. 2 Displacement ellipsoid plot (20% probability) of 2 at 100 K. Disorder C-atoms of TMC ring, anion and H-atoms have been removed for clarity.

chelated bi-dentate NO₃[−] anion (Fig. 2; ESI, ES, Fig. S4, Tables T1 and T2†).

OAT reaction of Co^{II}-nitrate complex (2)

So as to understand the NO₃[−] reduction chemistry of 2, we explored its reaction with VCl₃ to mimic the OAT based NRs enzymatic reaction. We observed a visible color change from pink to wine-red in the reaction of 2 with VCl₃ and a new absorption band (at 370 nm) formed, which is corresponding to the characteristic absorption band of a Co^{III}-nitrosyl ({CoNO})⁸, 4 (Fig. 3a and 6a).^{19d,20b,21a,27,30,32} Astonishingly, 2 upon reaction with VCl₃ generated corresponding Co^{III}-nitrosyl complex 4, ({CoNO})⁸,^{19d,20b,21a,27,30} with V^V-Oxo species in both aqueous/or methanol medium at 298 K (Scheme 1; reaction II). It is important to note that 2 did not show any spectral changes in the absence of VCl₃, suggesting that 2 is highly stable in H₂O/or MeOH and at 298 K (ESI, ES, and Fig. S5†). Finally, the product of NO₃[−] reduction, formed in the reaction of 2 and VCl₃, was established to be {CoNO}⁸ (4) based on various spectroscopic (UV-vis, FT-IR, ESI-MS, NMR) and structural characterization (*vide infra*).^{19d,20b,21a,27,30,32-33} The FT-IR spectrum of 2 showed a peak at 1384 cm^{−1}, characteristic to the Co^{II} bound NO₃[−] stretching frequency which shifted to 1703 cm^{−1} when 2 was reacted with VCl₃, which is characteristic of NO stretching frequency of {CoNO}⁸ (4).^{19d,20b,21a,27,30} The peak at 1703 cm^{−1} shifted to 1673 cm^{−1} when 4 was prepared by reacting ¹⁵N-labeled-NO₃[−] (Co^{II}-¹⁵NO₃[−]) with VCl₃, evidently suggesting the formation of {Co¹⁵NO}⁸ (inset: Fig. 3a; ESI and Fig. S6†). The shifting of NO stretching frequency ($\Delta = 30 \text{ cm}^{-1}$) indicates that N-atom in NO ligand is derived from Co^{II}-NO₃[−]. The ESI-MS spectrum of 4 showed a prominent peak at m/z 404.2, [(12-TMC)Co^{III}(NO)(BF₄)]⁺ (calcd m/z 404.2), and shifted to 405.2, [(12-TMC)Co^{III}(¹⁵NO)(BF₄)]⁺ (calcd m/z 405.2) when the reaction was performed with Co^{II}-¹⁵NO₃[−] (Fig. 3b; ESI, Fig. S7†); suggests clearly that NO moiety in 4 is derived from NO₃[−] moiety. The ¹H-NMR spectrum of 4 showed the peaks for the protons of 12-TMC ligand frameworks, confirming a low spin diamagnetic Co^{III} center (d^6 , $S = 0$) in complex 4 (ESI, Fig. S8†).^{32,33} Further, we have calculated the yield of 4 from NMR spectra using benzene as an internal standard and found to be 90 ± 3% (ESI, Fig. S9†).

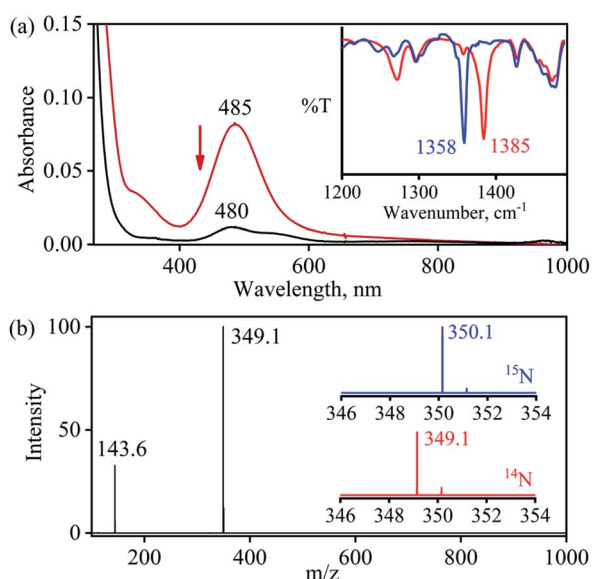


Fig. 1 (a) UV-vis spectra of 1 (0.50 mM, brick red line) and 2 (0.50 mM, black line) in CH₃CN under Ar at 298 K. Inset: IR spectra of 2-¹⁴NO₃[−] (red line) and 2-¹⁵NO₃[−] (blue line) in KBr. (b) ESI-MS spectra of 2. The peak at 349.1 is assigned to [(12TMC)Co^{II}(NO₃)]⁺ (calcd m/z 349.1). Inset: isotopic distribution pattern for 2-¹⁴NO₃[−] (red line) and 2-¹⁵NO₃[−] (blue line).

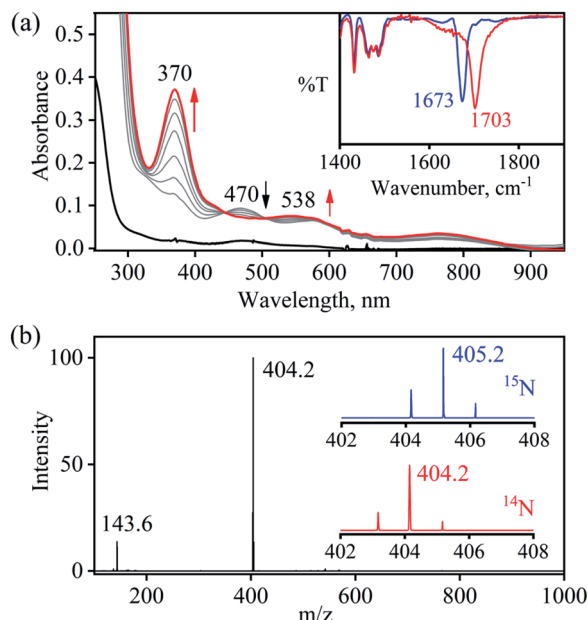


Fig. 3 (a) UV-vis spectral changes of **2** (0.50 mM, black line) upon addition of VCl_3 (2.2 equiv.) in H_2O at 298 K. Black line (**2**) changed to a red line (**4**) upon addition of VCl_3 . Inset: IR spectra **4**- ^{14}NO (blue line) and **4**- ^{15}NO (red line) in KBr. (b) ESI-MS spectra of **4**. The peak at 404.2 is assigned to $[(12\text{TMC})\text{Co}^{\text{III}}(\text{NO})(\text{BF}_4)]^+$ (calcd m/z 404.2). Inset: isotopic distribution pattern for **4**- ^{14}NO (red line) and **4**- ^{15}NO (blue line).

As a final point, the exact conformation of **4** was provided by its single-crystal X-ray crystallographic analysis (ESI, ES, Fig. S10, Tables T1 and T2†) and comparable with previously reported $\text{Co}^{\text{III}}\text{-NO}^-/\text{M-NO}^-$ having sp^2 hybridized N-atom.^{20b,21a,27,30,34} The lone pair present on N-atom is responsible for the significant bending of the $\text{Co}^{\text{III}}\text{-NO}^-$ moiety, with $\text{Co}(1)\text{-N}(5)\text{-O}(1)$ bond angles of 128.52 (18°) for **4** and, therefore, further consistent with the assignment of **4** as $\{\text{CoNO}\}^8$ species.

From the final spectrum (black line in Fig. 3a), we have calculated the amount of **4** ($90 \pm 2\%$) by comparing its ϵ ($\text{M}^{-1}\text{cm}^{-1}$) value at 370 nm, since $\text{V}^{\text{V}}\text{-Oxo}$ and VCl_3 species does not show any absorption at 370 nm. This value is also in good agreement with the yield calculated from NMR spectroscopy (ESI, Fig. S9†). Further, we had also determined the isolated yield of the formation of **4** and found it to be 90 (± 2)%, depicting clearly VCl_3 induced NO_3^- to NO transformation. The reduction of NO_3^- was observed to be slow; however, it enhanced with an increase in VCl_3 amount, suggesting that the NO_3^- to NO transformation follows the second-order reaction. Upon adding 10 equivalents of VCl_3 to the solution of **2** (0.5 mM), the UV-visible band at 370 nm starts forming with a pseudo-first-order rate constant, $k_{\text{obs}} = 1.2 \times 10^{-1} \text{ s}^{-1}$, and showed the isosbestic points at 418 and 497 nm (Fig. 3a). Upon increasing the concentration of VCl_3 , the pseudo-first-order rate constants increased proportionally, allowing us to determine a second-order rate constant (k_2) of $2.4 \times 10^{-2} \text{ M}^{-1} \text{ s}^{-1}$ (Fig. 4a) for the reaction of **2** with the various equivalents of VCl_3 (5, 10, 15, 20, 25).

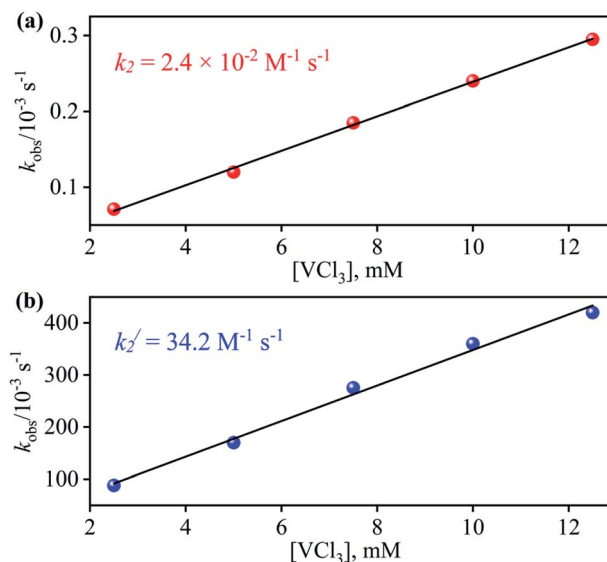


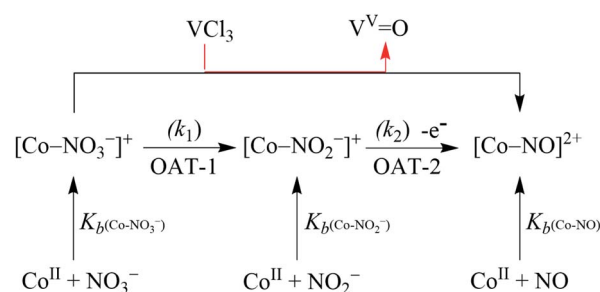
Fig. 4 Plot of k_{obs} versus the concentration of VCl_3 to determine the second order rate constant in the OAT reaction of (a) **2** (b) **3** in H_2O at 298 K.

Confirming $\text{V}^{\text{V}}\text{-Oxo}$ generation in NO_3^- reduction reaction via OAT

In order to authenticate our proposition of OAT promoted NO_3^- to NO reduction, we should observe the generation of $\text{V}^{\text{V}}\text{-Oxo}$ species during this transformation. In this regard, we have confirmed the conversion of VCl_3 to $\text{V}^{\text{V}}\text{-Oxo}$ species in the NO_3^- reduction reaction by ^{51}V -NMR. We observed the characteristic peaks of $\text{V}^{\text{V}}\text{-Oxo}$ species in the ^{51}V -NMR spectrum for the reaction mixture obtained after the completion of the reaction of **2** (4 mM) with VCl_3 (8 mM) in CD_3OD , at -365 , -525 , and -598 assignable to VOCl_3 , $\text{VOCl}(\text{OMe}_2)_2$ and $\text{VO}(\text{OMe}_2)_3$, respectively, as reported previously (ESI and Fig. S11†).³⁵ The observation of $\text{V}^{\text{V}}\text{-Oxo}$ species in the VCl_3 promoted NO_3^- reduction reaction indisputably illustrates that the VCl_3 sponsored NO_3^- to NO conversion should proceed via the two consecutive OAT reactions, where OAT-1 mimics the NRs enzymatic reaction,^{5b,36} while OAT-2 mimics the phosphorus or sulphur induced OAT transfer reactions (Schemes 1 and 2).^{26,31}

Mechanistic investigation of NO_3^- reduction

In the biological system, the conversion of NO_3^- to NO proceeds via a common NO_2^- intermediate in two consecutive steps (*vide*



Scheme 2

supra). In this report, it is dreadfully clear that the formation of NO from NO_3^- could only be accomplished *via* the VCl_3 induced two consecutive OAT reactions (*vide supra*), i.e., **OAT-1** & **OAT-2**. Hence, the conversion of NO_3^- to NO is likely to proceed *via* a $\text{Co}^{\text{II}}\text{-NO}_2^-$ intermediate (**3**). Although we were unable to isolate the intermediate **3**; however, we were able to show its generation by using VCl_3 as a limiting reagent (ES). In the reaction of **2** with 1.0-fold of VCl_3 , we observed the generation of **4** with $\text{Co}^{\text{II}}\text{-NO}_3^-$ and $\text{Co}^{\text{II}}\text{-NO}_2^-$ and confirmed with various spectroscopic measurements. The FT-IR spectrum of the above reaction mixture showed the characteristic peaks for $\text{Co}^{\text{II}}\text{-NO}_3^-$ (at 1385 cm^{-1}), $\text{Co}^{\text{II}}\text{-NO}_2^-$ (at 1272 cm^{-1}) and $\{\text{Co}^{14}\text{NO}\}^8$ (at 1703 cm^{-1}), those shifted to 1358 cm^{-1} , 1245 cm^{-1} and 1673 cm^{-1} when ^{15}N -labeled-nitrate complex ($3\text{-}^{15}\text{NO}_3^-$) reacted with VCl_3 , respectively (ESI, Fig. S12a and b†). Also, we have recorded the ESI-MS spectrum of the reaction mixture, which showed the prominent peaks at m/z 404.2, $[(12\text{-TMC})\text{Co}^{\text{III}}(\text{NO})(\text{BF}_4)]^+$ (calcd m/z 404.2), 333.1, $[(12\text{-TMC})\text{Co}^{\text{II}}(\text{NO}_2^-)]^+$ (calcd m/z 333.1) and $[(12\text{-TMC})\text{Co}^{\text{II}}(\text{NO}_3^-)]^+$ (calcd m/z 349.1), those shifted to 405.2, $[(12\text{-TMC})\text{Co}^{\text{III}}(^{15}\text{NO})(\text{BF}_4)]^+$ (calcd m/z 405.2), 334.1, $[(12\text{-TMC})\text{Co}^{\text{II}}(^{15}\text{NO}_2^-)]^+$ (calcd m/z 334.1) and $[(12\text{-TMC})\text{Co}^{\text{II}}(^{15}\text{NO}_3^-)]^+$ (calcd m/z 350.1), when the reaction was performed with $\text{Co}^{\text{II}}\text{-}^{15}\text{NO}_3^-$ and VCl_3 , respectively (ESI, Fig. S12c and d†). Further, when we reacted **2** with 1.5-fold of VCl_3 , we observed the generation of **4** with $\text{Co}^{\text{II}}\text{-NO}_2^-$ and confirmed by FT-IR and ESI-MS measurements. The FT-IR spectrum showed the characteristic peaks for $\text{Co}^{\text{II}}\text{-NO}_2^-$ (at 1272 cm^{-1}) and $\{\text{Co}^{14}\text{NO}\}^8$ (at 1703 cm^{-1}), and shifted to 1245 cm^{-1} ($\text{Co}^{\text{II}}\text{-}^{15}\text{NO}_2^-$) and 1673 cm^{-1} ($\{\text{Co}^{15}\text{NO}\}^8$) when using ^{15}N -labeled-nitrate complex ($3\text{-}^{15}\text{NO}_3^-$) (SI, Fig. S13a and b†). The ESI-MS spectrum, for the above reaction mixture, showed the prominent peaks at m/z 404.2, $[(12\text{-TMC})\text{Co}^{\text{III}}(\text{NO})(\text{BF}_4)]^+$ (calcd m/z 404.2), and 333.1, $[(12\text{-TMC})\text{Co}^{\text{II}}(\text{NO}_2^-)]^+$ (calcd m/z 333.2), and shifted to 405.2, $[(12\text{-TMC})\text{Co}^{\text{III}}(^{15}\text{NO})(\text{BF}_4)]^+$ (calcd m/z 405.2) and 333.1, $[(12\text{-TMC})\text{Co}^{\text{II}}(^{15}\text{NO}_2^-)]^+$ (calcd m/z 334.1), when using $\text{Co}^{\text{II}}\text{-}^{15}\text{NO}_3^-$ as starting reacting material in OAT reaction, correspondingly (ESI, Fig. S13d†). Together, the FT-IR and ESI-MS spectra confirmed that VCl_3 induced reduction of NO_3^- to NO is going through a $\text{Co}^{\text{II}}\text{-NO}_2^-$ (**3**) intermediate. Furthermore, as described above, when **2** reacted with 2.2-fold of VCl_3 , we had observed the generation of only complex **4** with nearly $90 \pm 2\%$ yield (*vide supra*).

With the intention of further validate our concept of $\text{Co}^{\text{II}}\text{-NO}_2^-$ species formation in the NO_3^- reduction reaction, in a control experiment, we explored the VCl_3 induced transformation of $\text{Co}^{\text{II}}\text{-NO}_2^-$ to one-electron oxidized $\{\text{CoNO}\}^8$ species;³⁷ possibly by the release of one electron which usually gets solvated as observed in other cases,³⁸ and trailed the fate of OAT reaction (Fig. 5). For this reaction, the initial $\text{Co}^{\text{II}}\text{-NO}_2^-$ complex was prepared by following the reported literature (Scheme 1, reaction **Vla**).^{21a,27} Upon addition of one fold VCl_3 to a solution of **3** in $\text{MeOH}/\text{H}_2\text{O}$ at RT, the color of the reaction solution immediately changed from light pink to wine red, suggesting the generation of $\{\text{CoNO}\}^8$ (**4**),³⁷ and its characteristic absorption band (at 370 nm) appeared in ~ 1 minute as shown in Fig. 5 and 6b (Scheme 1, reaction **Vib**). Also, we have calculated the yield of **4** by comparing its ϵ ($\text{M}^{-1}\text{ cm}^{-1}$) value at

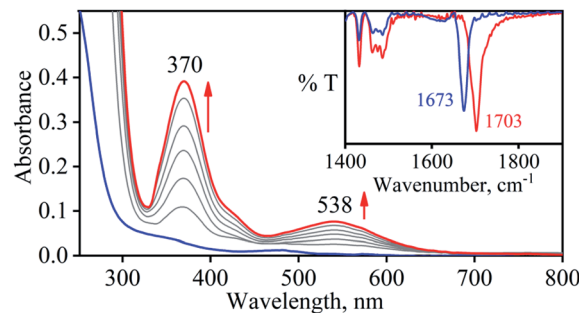


Fig. 5 UV-vis spectral changes of **3** (0.50 mM, blue line) upon addition of VCl_3 (1 equiv.) in H_2O at 298 K. Blue line (**3**) changed to red line (**4**) upon addition of VCl_3 . Inset: IR spectra $4\text{-}^{14}\text{NO}$ (blue line) and $4\text{-}^{15}\text{NO}$ (red line) in KBr.

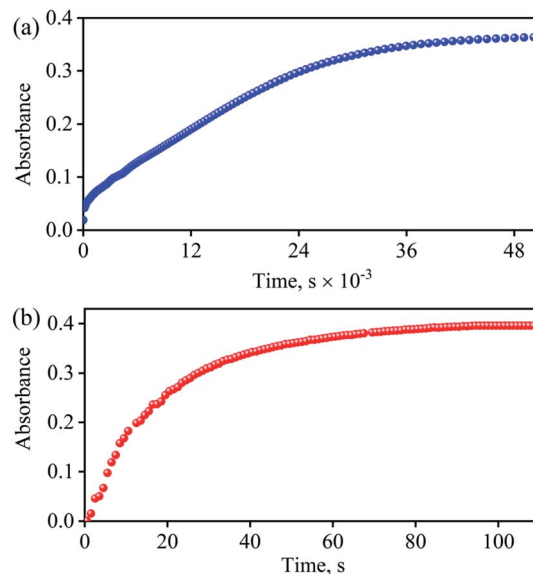


Fig. 6 (a) Time course of the formation of **4** (blue circles) monitored at 370 nm upon addition VCl_3 (2.2 equiv.) to a solution of **2** (0.5 mM) in H_2O at 298 K. (b) Time course of the formation of **4** (Red circles) monitored at 370 nm upon addition VCl_3 (1 equiv.) to a solution of **3** (0.5 mM) in H_2O at 298 K.

370 nm and found it to be ($>95 \pm 2\%$). Further, spectral titration data confirmed that the stoichiometric ratio of **3** with VCl_3 was 1 : 1 (ESI, Fig. S14†). Furthermore, the final product (**4**) was confirmed by the FT-IR and ^1H -NMR spectroscopy (ESI, Fig. S15 and S16†).^{19d,20b,21a,27,30} Also, the generation of V^{V} -Oxo species was confirmed by the ^{51}V -NMR (ESI, Fig. S17†). Speedy conversion of **3** to **4** in the presence of VCl_3 justifies our inability to isolate intermediate **3** in the VCl_3 induced conversion of **2** to **4** and supports our supposition of two consecutive OAT reactions in reducing NO_3^- to NO. We have also determined the second-order rate constant for the reduction of NO_2^- to NO to understand the reaction mechanism and NO formation fate. The second-order rate constant (k_2') for NO_2^- reduction was determined by plotting the pseudo-first-order rate constant against various equivalents of VCl_3 (5, 10, 15, 20, and 25) and found to be $34.2\text{ M}^{-1}\text{ s}^{-1}$ (Fig. 4b). Our efforts to isolate the $\text{Co}^{\text{II}}\text{-NO}_2^-$

intermediate in the NO_3^- reduction reaction is unsuccessful due to the high reactivity of $\text{Co}^{\text{II}}\text{-NO}_2^-$ with VCl_3 (**OAT-2**), which is ~ 1420 times faster than the second-order rate constant of VCl_3 induced NO_3^- to NO reduction ($k_2 = 2.4 \times 10^{-2} \text{ M}^{-1} \text{ s}^{-1}$).

Spectroscopic and kinetic measurements undeniably confirmed that the reaction of **3** with VCl_3 generates **4** ($\{\text{CoNO}\}^8$) plus $\text{V}^{\text{V}}\text{-Oxo}$ species with a second-order rate constant ($k_2' = 34.2 \text{ M}^{-1} \text{ s}^{-1}$), suggesting a rapid conversion (Fig. 6b). However, the transformation of **2** to **4** was observed to be a prolonged reaction, based on the spectral measurements (*vide infra*), in two sequential OAT reactions with a second-order rate-constant ($k_2 = 2.4 \times 10^{-2} \text{ M}^{-1} \text{ s}^{-1}$) *via* a $\text{Co}^{\text{II}}\text{-NO}_2^-$ intermediate. This comparison of rate constants ($k_2 \ll k_2'$) suggests that the formation of NO_2^- from NO_3^- is a rate-determining step in the NO_3^- to NO reduction chemistry. Kinetic measurements (*vide supra*) confirmed clearly that the first step of the reaction (Scheme 1, pathway II) is the slowest step of the reaction; hence, a rate-determining step. Therefore, the overall second-order rate constant ($k_2 = 2.4 \times 10^{-2} \text{ M}^{-1} \text{ s}^{-1}$) is equal to the rate constant of the conversion of **2** to **3** (Fig. 4a and 6a). Additionally, the binding constants ($K_{\text{b}(\text{Co}^{\text{II}}\text{-NO}_3^-)}$, $K_{\text{b}(\text{Co}^{\text{II}}\text{-NO}_2^-)}$, & $K_{\text{b}(\{\text{CoNO}\}^8)}$) for the generation of different species, $\text{Co}^{\text{II}}\text{-NO}_3^-$, $\text{Co}^{\text{II}}\text{-NO}_2^-$ & $\{\text{CoNO}\}^8$ in the reaction of $[\text{Co}^{\text{II}}(\text{CH}_3\text{CN})(12\text{TMC})]^{2+}$ with NO_3^- , NO_2^- & NO , were determined by using Benesi–Hildebrand equation³⁹ and found to be $2.3 \times 10^2 \text{ M}^{-1}$, $2.5 \times 10^3 \text{ M}^{-1}$ & $2.4 \times 10^3 \text{ M}^{-1}$ (ESI, ES, and Fig. S18†), respectively (Scheme 2). Structural parameters and ambiphilic nature of O-atom in coordinated NO_3^- & NO_2^- species, in their respective complexes,²⁸ and the binding constants calculations further support our proposal of two OAT reactions with different reaction rates ($r_2 \gg r_1$). The $K_{\text{b}(\text{Co}^{\text{II}}\text{-NO}_2^-)}$ is higher than that of $K_{\text{b}(\text{Co}^{\text{II}}\text{-NO}_3^-)}$; hence the reaction moves in the forward direction once the NO_2^- generates from NO_3^- in **OAT-1**. However, the abstraction of the first non-coordinated O-atom from NO_3^- using VCl_3 is somewhat hard due to its less electrophilic nature and more bond strength (bond length $_{\text{(N-O)}} = 1.215 \text{ \AA}$) compare to other more electrophilic Co^{2+} -coordinated O-atoms (bond length $_{\text{(N-O)}} = 1.267 \text{ \AA}$ & 1.269 \AA); therefore showed a slower rate of **OAT-1** (r_1) than **OAT-2** (r_2) reaction, as proposed theoretically in CO induced Ni- NO_3^- reduction chemistry, suggesting the slow rate of NO_3^- to NO_2^- than NO_2^- to NO .²⁸ Kim and co-workers reported that the alteration of O-atom's electrophilic behavior in NO_3^- species, induced by the Sc^{3+} metal (Lewis acid) binding, showed the NO_3^- to NO_2^- reduction, which was not observed in the absence of Sc^{3+} ion, suggesting the O-atom activation upon Sc^{3+} binding. Discussion on the OAT chemistry²⁸ and metal-induced activation of O-atom²⁴ (*vide supra*) undoubtedly support our supposition of a faster **OAT-2** than the **OAT-1**, as non-co-ordinated O-atom of NO_3^- is difficult to abstract by VCl_3 than Co^{2+} -co-ordinated O-atoms of nitrite moiety.^{24,28} Recent reports on Lewis acid induced OAT reactions showed an increase in the oxidizing power of M-oxygen adducts and their OAT reaction rate,⁴⁰ which coincides with the activation of N_2 by Lewis acid.^{28,41} Further, the difference in the rates of the NO_3^- & NO_2^- reduction were supported by the inert and labile behavior of Co-complexes. High spin Co^{II} -complexes, **2** and **3**, are labile (d^7 , $S = 3/2$);⁴² hence the conversion of **2** to **3**

was found to be slow as there is not much change in the CFSE; however, the conversion of labile **3** to an inert **4** (d^6 , $S = 0$) found to be very fast as there is a huge change in the CFSE, in order to achieve more stable inert electronic configuration.^{19d,43} These results verify our theory of step-wise conversion of NO_3^- to NO_2^- , which further reduces to NO in the presence of VCl_3 in two consecutive OAT reactions.

Conclusion

Investigation of insights into the mechanistic aspects of the NO_3^- & NO_2^- reduction process became a most significant research area in modern-day chemistry as it deals with the biological and environmental aspects.¹ Reduction of NO_3^- to NO *via* NO_2^- intermediate species are key steps in biological NO generation (salivary NRs followed by NiRs in mammalian system)^{5,44} and also for the denitrification process (biogeochemical systems).^{1,45} Reduction of NO_3^- to NO using a single metal complex is still a challenge to the scientific community as two different enzymes play the catalytic role in each step in the biological system.^{2,3} In this report, for the very first time, we have shown the direct reduction of NO_3^- in a Co^{II} -nitrate complex, $[(12\text{TMC})\text{Co}^{\text{II}}(\text{NO}_3^-)]^+$ (**2**), to a Co-nitrosyl complex $\{\text{CoNO}\}^8$ (**4**), in the presence of an oxophilic reagent (VCl_3). Mechanistic investigation suggests that the reaction proceeds *via* a $\text{Co}^{\text{II}}\text{-NO}_2^-$ (**3**) species, as observed in the case of biological NRs enzymatic chemistry,⁵ in two consecutive OAT reactions. Kinetic measurements suggest that the VCl_3 induced reduction of NO_3^- to NO_2^- is a rate-determining step ($k_2 = 2.4 \times 10^{-2}$, **OAT-1**), mimicking the salivary molybdate NRs enzymatic reaction.⁵ In the second step (**OAT-2**), a speedy reduction process ($k_2' = 34.2$), NO_2^- further reduces to NO in the presence of one-fold VCl_3 . Isolation of **3** was difficult due to the fast conversion of **3** to **4**; however, we could characterize it with various spectroscopic techniques. The results observed in VCl_3 induced NO_3^- reduction to NO in two consecutive OAT reactions are found to be in good agreement with our proposed concept. The results are explained in the light of the bond strength and the electrophilic behavior of O-atoms of $\text{NO}_3^-/\text{NO}_2^-$ ligands and based on the inert & labile nature of Co-complexes. Due to high bond strength and less electrophilic character of metal-unbound O-atom of NO_3^- , it showed a slower OAT reaction (r_1); in contrast, O-atoms of NO_2^- moiety is activated due to their binding with Co^{II} -center, and the OAT from NO_2^- to VCl_3 found to be very fast (r_2), as observed in Ni- NO_3^- reduction chemistry.²⁸ Also, the conversion of high spin **2** to **3** (d^7 , $S = 3/2$) is slow due to a very less change in the CFSE compare to the transformation of high spin **3** to a low spin **4** (d^6 , $S = 0$) with much change in the CFSE, additionally support our chemistry. Furthermore, direct generation of **4** from **3** supports our proposition that $\text{Co}^{\text{II}}\text{-NO}_2^-$ involved as an intermediate species in NO_3^- to NO transformation. Tracking the reactions using ^{15}N -labeled- $^{15}\text{NO}_3^-$ and $^{15}\text{NO}_2^-$ evidently suggests that the N-atom in the $\{\text{CoNO}\}^8$ species is derived from NO_3^- moiety. N–O bond activation^{20b,21a,27,30,34a,34c} of coordinated NO_3^- in **2** generates **4**,^{19d} hence implying that the OAT reaction of **2** in the presence of VCl_3 generates the Co-nitrosyl species. This work highlights the



first-ever report of VCl_3 encouraged the reduction of NO_3^- to NO_2^- (NRs activity, **OAT-1**) followed by another OAT induced NO_2^- to NO transformation (**OAT-2**). In nature, both the reduction process needs two different enzymes for converting NO_3^- to NO; hence, the proposed OAT reagent (VCl_3), which is capable of doing the same in a one-shot, has border significance with respect to biological as well as environmental systems.

Author contributions

PKK & Kulbir discovered/conceptualized the initial project. Kulbir, SD, MG, PB, & MY carried out the different experiments and gathered the data. PKK, SG & TD helped in interpreting the experimental results. Kulbir and SD write the first draft of the article. PKK & TD have corrected the manuscript, finalized the final draft, and guided during the revision. PKK followed and guided the whole project work.

Conflicts of interest

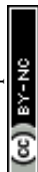
There are no conflicts to declare.

Acknowledgements

This work was supported by Grants-in-Aid (Grant No. EEQ/2016/000466) from SERB-DST. KK, SD, MY, PB, and SG thank IISER Tirupati for financial assistance and for providing the research facility. SCS thanks DST-FIST for the single crystal facility at PU. Special thanks to Prof. K. Vijayamohanan Pillai (IISER Tirupati) for fruitful discussion and support.

References

- 1 P. Tavares, A. S. Pereira, J. J. Moura and I. Moura, *J. Inorg. Biochem.*, 2006, **100**, 2087–2100.
- 2 E. Weitzberg and J. O. Lundberg, *Nitric Oxide*, 1998, **2**, 1–7.
- 3 J. O. Lundberg and M. Govoni, *Free Radical Biol. Med.*, 2004, **37**, 395–400.
- 4 (a) L. Ma, L. Hu, X. Feng and S. Wang, *Aging Dis.*, 2018, **9**, 938–945; (b) G. M. McKnight, C. W. Duncan, C. Leifert and M. H. Golden, *Br. J. Nutr.*, 1999, **81**, 349–358; (c) M. J. Hill, G. Hawke and G. Tattersall, *Br. J. Cancer*, 1973, **28**, 562–567; (d) L. Juhasz, M. J. Hill and G. Nagy, *IARC Sci. Publ.*, 1980, 619–623; (e) O. M. Jensen, *Ecotoxicol. Environ. Saf.*, 1982, **6**, 258–267; (f) C. J. Johnson and B. C. Kross, *Am. J. Ind. Med.*, 1990, **18**, 449–456.
- 5 (a) L. I. Hochstein and G. A. Tomlinson, *Annu. Rev. Microbiol.*, 1988, **42**, 231–261; (b) W. H. Campbell, *Annu. Rev. Plant Physiol. Plant Mol. Biol.*, 1999, **50**, 277–303.
- 6 N. Benjamin, F. O'Driscoll, H. Dougall, C. Duncan, L. Smith, M. Golden and H. McKenzie, *Nature*, 1994, **368**, 502.
- 7 J. O. Lundberg, E. Weitzberg, J. M. Lundberg and K. Alving, *Gut*, 1994, **35**, 1543–1546.
- 8 B. A. Averill, *Chem. Rev.*, 1996, **96**, 2951–2964.
- 9 E. I. Tocheva, F. I. Rosell, A. G. Mauk and M. E. Murphy, *Science*, 2004, **304**, 867–870.
- 10 R. B. S. Nabi, R. Tayade, A. Hussain, K. P. Kulkarni, Q. M. Imran, B.-G. Mun and B.-W. Yun, *Environ. Exp. Bot.*, 2019, **161**, 120–133.
- 11 (a) R. F. Furchgott, *Angew. Chem., Int. Ed.*, 1999, **38**, 1870–1880; (b) L. J. Ignarro, *Angew. Chem., Int. Ed.*, 1999, **38**, 1882–1892; (c) L. J. Ignarro, *Nitric oxide: biology and pathobiology*, Academic press, 2000; (d) G. B. Richter-Addo, P. Legzdins and J. Burstyn, *Chem. Rev.*, 2002, **102**, 857–860; (e) I. M. Wasser, S. de Vries, P. Moënné-Loccoz, I. Schröder and K. D. Karlin, *Chem. Rev.*, 2002, **102**, 1201–1234.
- 12 F. Vargas, J. M. Moreno, R. Wangenstein, I. Rodriguez-Gomez and J. Garcia-Estan, *Eur. J. Endocrinol.*, 2007, **156**, 1–12.
- 13 (a) P. Pacher, J. S. Beckman and L. Liaudet, *Physiol. Rev.*, 2007, **87**, 315–424; (b) R. Radi, *Proc. Natl. Acad. Sci. U. S. A.*, 2004, **101**, 4003–4008; (c) B. Kalyanaraman, *Proc. Natl. Acad. Sci. U. S. A.*, 2004, **101**, 11527–11528; (d) P. C. Dedon and S. R. Tannenbaum, *Arch. Biochem. Biophys.*, 2004, **423**, 12–22.
- 14 (a) R. E. Huie and S. Padmaja, *Free Radical Res. Commun.*, 1993, **18**, 195–199; (b) C. Prolo, M. N. Alvarez and R. Radi, *Biofactors*, 2014, **40**, 215–225.
- 15 (a) W. C. Nottingham and J. R. Sutter, *Int. J. Chem. Kinet.*, 1986, **18**, 1289–1302; (b) C. H. Lim, P. C. Dedon and W. M. Deen, *Chem. Res. Toxicol.*, 2008, **21**, 2134–2147.
- 16 (a) D. D. Thomas, L. A. Ridnour, J. S. Isenberg, W. Flores-Santana, C. H. Switzer, S. Donzelli, P. Hussain, C. Vecoli, N. Paolocci, S. Ambs, C. A. Colton, C. C. Harris, D. D. Roberts and D. A. Wink, *Free Radical Biol. Med.*, 2008, **45**, 18–31; (b) D. L. Granger and J. B. Hibbs Jr, *Trends Microbiol.*, 1996, **4**, 46–47; (c) C. F. Nathan and J. B. Hibbs Jr, *Curr. Opin. Immunol.*, 1991, **3**, 65–70.
- 17 N. Lehnert, T. C. Berto, M. G. I. Galinato and L. E. Goodrich, in *Handbook of Porphyrin Science*, ed. K. Kadish, K. Smith and R. Guilard, World Scientific Publishing, Singapore, 2011, p. 1.
- 18 (a) T. B. McCall, N. K. Boughton-Smith, R. M. Palmer, B. J. Whittle and S. Moncada, *Biochem. J.*, 1989, **261**, 293–296; (b) R. G. Knowles and S. Moncada, *Biochem. J.*, 1994, **298**(Pt 2), 249–258.
- 19 (a) P. C. Ford and I. M. Lorkovic, *Chem. Rev.*, 2002, **102**, 993–1018; (b) M. P. Schopfer, B. Mondal, D. H. Lee, A. A. Sarjeant and K. D. Karlin, *J. Am. Chem. Soc.*, 2009, **131**, 11304–11305; (c) M. P. Doyle and J. W. Hoekstra, *J. Inorg. Biochem.*, 1981, **14**, 351–358; (d) M. Yenuganti, S. Das, Kulbir, S. Ghosh, P. Bhardwaj, S. S. Pawar, S. C. Sahoo and P. Kumar, *Inorg. Chem. Front.*, 2020, **7**, 4872–4882.
- 20 (a) S. G. Clarkson and F. Basolo, *Inorg. Chem.*, 1973, **12**, 1528–1534; (b) P. Kumar, Y. M. Lee, Y. J. Park, M. A. Siegler, K. D. Karlin and W. Nam, *J. Am. Chem. Soc.*, 2015, **137**, 4284–4287; (c) K. Gogoi, S. Saha, B. Mondal, H. Deka, S. Ghosh and B. Mondal, *Inorg. Chem.*, 2017, **56**, 14438–14445; (d) G. Y. Park, S. Deepalatha, S. C. Pui, D. H. Lee, B. Mondal, A. A. Narducci Sarjeant, D. del Rio, M. Y. Pau, E. I. Solomon and K. D. Karlin, *J. Biol. Inorg. Chem.*, 2009, **14**, 1301–1311; (e) A. Yokoyama, K. B. Cho, K. D. Karlin and W. Nam, *J. Am. Chem. Soc.*, 2013, **135**,



- 14900–14903; (f) S. Hong, P. Kumar, K. B. Cho, Y. M. Lee, K. D. Karlin and W. Nam, *Angew. Chem., Int. Ed. Engl.*, 2016, **55**, 12403–12407; (g) A. Yokoyama, J. E. Han, K. D. Karlin and W. Nam, *Chem. Commun.*, 2014, **50**, 1742–1744; (h) A. Kalita, P. Kumar and B. Mondal, *Chem Commun.*, 2012, **48**, 4636–4638.
- 21 (a) S. Das, Kulbir, S. Ghosh, S. Chandra Sahoo and P. Kumar, *Chem. Sci.*, 2020, **11**, 5037–5042; (b) F. Roncaroli, L. M. Baraldo, L. D. Slep and J. A. Olabe, *Inorg. Chem.*, 2002, **41**, 1930–1939; (c) A. Kalita, P. Kumar, R. C. Deka and B. Mondal, *Chem Commun.*, 2012, **48**, 1251–1253.
- 22 J. Jiang and R. H. Holm, *Inorg. Chem.*, 2005, **44**, 1068–1072.
- 23 A. Majumdar, K. Pal and S. Sarkar, *J. Am. Chem. Soc.*, 2006, **128**, 4196–4197.
- 24 L. T. Elrod and E. Kim, *Inorg. Chem.*, 2018, **57**, 2594–2602.
- 25 C. Khin, J. Heinecke and P. C. Ford, *J. Am. Chem. Soc.*, 2008, **130**, 13830–13831.
- 26 S. Kundu, W. Y. Kim, J. A. Bertke and T. H. Warren, *J. Am. Chem. Soc.*, 2017, **139**, 1045–1048.
- 27 M. A. Puthiyaveetil Yoosaf, S. Ghosh, Y. Narayan, M. Yadav, S. C. Sahoo and P. Kumar, *Dalton Trans.*, 2019, **48**, 13916–13920.
- 28 J. Gwak, S. Ahn, M. H. Baik and Y. Lee, *Chem. Sci.*, 2019, **10**, 4767–4774.
- 29 J. A. Halfen and W. B. Tolman, *J. Am. Chem. Soc.*, 1994, **116**, 5475–5476.
- 30 P. Kumar, Y. M. Lee, L. Hu, J. Chen, Y. J. Park, J. Yao, H. Chen, K. D. Karlin and W. Nam, *J. Am. Chem. Soc.*, 2016, **138**, 7753–7762.
- 31 (a) L. Cheng, M. A. Khan, G. B. Richter-Addo and D. R. Powell, *Chem Commun.*, 2000, 2301–2302, DOI: 10.1039/b006775j; (b) A. K. Patra, R. K. Afshar, J. M. Rowland, M. M. Olmstead and P. K. Mascharak, *Angew. Chem., Int. Ed.*, 2003, **42**, 4517–4521; (c) B. C. Sanders, S. M. Hassan and T. C. Harrop, *J. Am. Chem. Soc.*, 2014, **136**, 10230–10233; (d) T. S. Kurtikyan, A. A. Hovhannisyan, A. V. Iretskii and P. C. Ford, *Inorg. Chem.*, 2009, **48**, 11236–11241.
- 32 P. Kumar, Y. M. Lee, L. Hu, J. Chen, Y. J. Park, J. Yao, H. Chen, K. D. Karlin and W. Nam, *J. Am. Chem. Soc.*, 2016, **138**, 7753–7762.
- 33 P. Kumar, Y. M. Lee, Y. J. Park, M. A. Siegler, K. D. Karlin and W. Nam, *J. Am. Chem. Soc.*, 2015, **137**, 4284–4287.
- 34 (a) C. Uyeda and J. C. Peters, *J. Am. Chem. Soc.*, 2013, **135**, 12023–12031; (b) M. R. Walter, S. P. Dzulf, A. V. Rodrigues, T. L. Stemmler, J. Telser, J. Conradie, A. Ghosh and T. C. Harrop, *J. Am. Chem. Soc.*, 2016, **138**, 12459–12471; (c) Y. Guo, J. R. Stroka, B. Kandemir, C. E. Dickerson and K. L. Bren, *J. Am. Chem. Soc.*, 2018, **140**, 16888–16892; (d) C. H. Chuang, W. F. Liaw and C. H. Hung, *Angew. Chem., Int. Ed.*, 2016, **55**, 5190–5194.
- 35 (a) O. W. Howarth, *Prog. Nucl. Magn. Reson. Spectrosc.*, 1990, **22**, 453–485; (b) D. Rehder, *Bull. Magn. Reson.*, 1982, **4**, 33–83.
- 36 W. H. Campbell, *Cell. Mol. Life Sci.*, 2001, **58**, 194–204.
- 37 The product of VCl₃ induced OAT-2 reaction is {CoNO}⁸ not {CoNO}⁹, suggesting a missing electron in the Co–NO₂[–] reduction reaction. One electron loss has been shown in the Scheme 1 and 2 for better understanding, which probably solvated in presence of excess solvent. As a tiny entity, it is very challenging to track an electron in the system. As there is a missing electron in the overall NO₂[–] reduction reaction, we did not describe a more detailed mechanism and based on the product analysis, we proposed the OAT transfer from NO₂[–] moiety.
- 38 (a) K. R. Siefermann, Y. Liu, E. Lugovoy, O. Link, M. Faubel, U. Buck, B. Winter and B. Abel, *Nat. Chem.*, 2010, **2**, 274–279; (b) C. R. Wang, J. Nguyen and Q. B. Lu, *J. Am. Chem. Soc.*, 2009, **131**, 11320–11322; (c) L. Sanche, *Nature*, 2009, **461**, 358–359; (d) V. Petrosyan, M. E. Niyazymbetov, é. V. Ulyanov and U. Niyazymbetov, *Division of chemical science*, 1989, **38**, 1548–1551.
- 39 (a) S. Goswami, D. Sen, N. K. Das, H. K. Fun and C. K. Quah, *Chem Commun.*, 2011, **47**, 9101–9103; (b) J. Chen, H. Yoon, Y. M. Lee, M. S. Seo, R. Sarangi, S. Fukuzumi and W. Nam, *Chem. Sci.*, 2015, **6**, 3624–3632; (c) Y. M. Lee, M. Yoo, H. Yoon, X. X. Li, W. Nam and S. Fukuzumi, *Chem Commun.*, 2017, **53**, 9352–9355.
- 40 S. Fukuzumi, K. Ohkubo, Y.-M. Lee and W. Nam, *Chem. -Eur. J.*, 2015, **21**, 17548–17559.
- 41 J. B. Geri, J. P. Shanahan and N. K. Szymczak, *J. Am. Chem. Soc.*, 2017, **139**, 5952–5956.
- 42 H. Taube, *Chem. Rev.*, 1952, **50**, 69–126.
- 43 G. L. Miessler, P. J. Fischer and D. A. Tarr, *Inorganic Chemistry*, Pearson, 5th edn, 2014.
- 44 B. A. Averill, *Chem. Rev.*, 1996, **96**, 2951–2964.
- 45 A. Tilstra, Y. C. El-Khaled, F. Roth, N. Radecker, C. Pogoreutz, C. R. Voolstra and C. Wild, *Sci. Rep.*, 2019, **9**, 19460.

